PNAS RESEARCH ARTICLE | CELL BIOLOGY

FOXO-mediated repression of Dicer1 regulates metabolism, stress resistance, and longevity in *Drosophila*

Juan A. Sánchez[a,1], María C. Ingaramo[a,1], María P. Gervé[a], Maria G. Thomas[b], Graciela L. Boccaccio[b,c], and Andrés Dekanty[a,d,2]

Edited by Gary Ruvkun, Massachusetts General Hospital, Boston, MA; received September 27, 2022; accepted March 4, 2023

The adipose tissue plays a crucial role in metabolism and physiology, affecting animal lifespan and susceptibility to disease. In this study, we present evidence that adipose Dicer1 (Dcr-1), a conserved type III endoribonuclease involved in miRNA processing, plays a crucial role in the regulation of metabolism, stress resistance, and longevity. Our results indicate that the expression of Dcr-1 in murine 3T3L1 adipocytes is responsive to changes in nutrient levels and is subject to tight regulation in the *Drosophila* fat body, analogous to human adipose and hepatic tissues, under various stress and physiological conditions such as starvation, oxidative stress, and aging. The specific depletion of Dcr-1 in the *Drosophila* fat body leads to changes in lipid metabolism, enhanced resistance to oxidative and nutritional stress, and is associated with a significant increase in lifespan. Moreover, we provide mechanistic evidence showing that the JNK-activated transcription factor FOXO binds to conserved DNA-binding sites in the *dcr-1* promoter, directly repressing its expression in response to nutrient deprivation. Our findings emphasize the importance of FOXO in controlling nutrient responses in the fat body by suppressing Dcr-1 expression. This mechanism coupling nutrient status with miRNA biogenesis represents a novel and previously unappreciated function of the JNK-FOXO axis in physiological responses at the organismal level.

Drosophila | miRNA | oxidative stress | adipose tissue | dicer-1

Significance

The adipose tissue plays an essential role in regulating metabolism and physiology, which has a significant impact on animal lifespan and disease susceptibility. Here, we provide evidence that adipose Dicer1, a conserved type III endoribonuclease involved in miRNA processing, plays a key role in the regulation of metabolism, stress resistance, and longevity. We also show that FOXO-mediated repression of Dicer1 in the *Drosophila* fat body, a functional analog of vertebrate adipose and hepatic tissues, is necessary for maintaining metabolic homeostasis and extending animal survival under nutrient deprivation. These findings demonstrate the critical role that the adipose tissue and the FOXO-Dicer1 axis play in regulating metabolism, physiology, and health.

The adipose tissue has recently been recognized as a crucial organ in the regulation of metabolism, lifespan, and disease susceptibility. Previous results have suggested that microRNAs (miRNAs) are essential in the adipose tissue for the regulation of various metabolic processes and for the adaptation to challenging nutrient conditions (1, 2). Dicer1 (Dcr-1), a conserved type III endoribonuclease involved in miRNA processing, has been identified in the adipose tissue of both mice and *Drosophila* as a rate-limiting enzyme in the biogenesis of miRNAs (3, 4). As mice age, Dicer1 levels in this specific organ decrease causing a reduction in miRNA processing (4, 5). This global decline in adipose miRNA levels is alleviated by caloric restriction, a well-known antiaging diet (5). The expression of Dicer1 in the adipose tissue is also downregulated in response to obesity and HIV-related lipodystrophy (6). Interestingly, adipose-specific Dicer1 knockout mice developed insulin resistance and hyperglycemia when subjected to a high-fat diet, suggesting that downregulation of Dicer1 in adipose tissue contributes to aging and age-associated type-2 diabetes (6). However, aerobic exercise upregulates Dicer1 expression and overall miRNA levels, these being required for controlled substrate utilization in the adipose tissue and therefore whole-body metabolic adaptations to aerobic exercise (7). Further studies concerning adipose Dcr-1 function in the adaptation at an organismal level to different nutrient and metabolic challenges will contribute to a better understanding of miRNA processing and Dcr-1 roles in animal physiology, aging, and disease.

The *Drosophila* fat body (FB), a functional analog of adipose and hepatic tissues in vertebrates, is implicated in energy storage and expenditure, nutrient sensing and the regulation of animal lifespan (8–11). In a previous study, we demonstrated that Dcr-1 and miRNAs processing are downregulated in the FB of starved flies, both events necessary for whole-organism adaptation to fasting conditions (3). Reduced Dcr-1 levels and impaired miRNA biogenesis under nutrient stress activate the *Drosophila* ortholog of mammalian p53 (Dmp53) which in turn promotes survival by repression of systemic insulin signaling and the maintenance of energy stores (3, 12). Here, we provide evidence of a critical role of Dcr-1 in regulating metabolism, stress resistance, and longevity in *Drosophila*. We showed that Dcr-1 expression is tightly regulated in the fat body under several stress-inducing and physiological conditions including starvation, oxidative stress and aging, and nutrient-dependent regulation of Dcr-1 levels is conserved in murine 3T3L1 adipocytes. Fat body-specific depletion of Dcr-1 leads to alterations in glucose and energy homeostasis and increased viability in response to starvation conditions and oxidative stress. In addition, we showed that JNK-dependent activation of the transcription

Author affiliations: [a]Instituto de Agrobiotecnología del Litoral, Consejo Nacional de Investigaciones Científicas y Técnicas, Santa Fe 3000, Argentina; [b]Instituto de Investigaciones Bioquímicas de Buenos Aires, Consejo Nacional de Investigaciones Científicas y Técnicas and Instituto Leloir, Buenos Aires 1405, Argentina; [c]Facultad de Ciencias Exactas y Naturales, Universidad de Buenos Aires, Buenos Aires 1428, Argentina; and [d]Facultad de Bioquímica y Ciencias Biológicas, Universidad Nacional del Litoral, Santa Fe 3000, Argentina

Author contributions: A.D. designed research; J.A.S., M.C.I., and M.P.G. performed research; J.A.S., M.C.I., and A.D. analyzed data; M.G.T. and G.L.B. provided starved 3T3-L1 cells; and M.C.I. and A.D. wrote the paper.

The authors declare no competing interest.

This article is a PNAS Direct Submission.

[1]J.A.S. and M.C.I. contributed equally to this work.

[2]To whom correspondence may be addressed. Email: adekanty@santafe-conicet.gov.ar.

This article contains supporting information online at https://www.pnas.org/lookup/suppl/doi:10.1073/pnas.2216539120/-/DCSupplemental.

Published April 4, 2023.

factor FOXO represses *dcr-1* expression in the adipose tissue upon nutrient deprivation, thus impairing miRNA processing. Chromatin immunoprecipitation (ChIP) assays revealed that FOXO binds to canonical DNA-binding sites located in the *dcr-1* promoter region thus directly repressing *dcr-1* transcription under starvation. Interestingly, FOXO-mediated *dcr-1* repression is required for extending survival rates under nutrient deprivation. These findings demonstrate that FOXO-dependent repression of Dcr-1 in adipose cells is required for maintaining metabolic homeostasis and extending animal survival under nutrient stress.

Results

Fat Body-Specific Role of Dcr-1 in Stress Resistance and Metabolic Homeostasis. As described in previous studies, the regulation of *dcr-1* transcript levels by nutrient availability was observed in the FB and showed a strong reduction after 24 h of starvation (STV) treatment [Fig. 1*A*; (3)]. A decrease in *dcr-1* levels was also observed in larval carcass, mainly comprising epidermis, muscles, and oenocytes (*SI Appendix*, Fig. S1). Conversely, the transcript analysis of *dcr-1* levels in the larval brain and intestine showed no changes upon STV (*SI Appendix*, Fig. S1). To determine whether nutrient-dependent regulation of *dcr-1* levels is conserved in vertebrates, we exposed differentiated murine 3T3L1 cells (white adipocytes) to serum deprivation. As shown in Fig. 1*C*, there was a significant reduction in *dicer1* transcript levels immediately after 1 h of STV. To examine whether reduced adipose *dcr-1* levels actually compromise miRNAs processing in *Drosophila,* we measured the levels of miRNAs known to be highly expressed in the FB. As expected, mature miR-8 and miR-305 levels were reduced in the FB of starved animals (Fig. 1*B*), and *dcr-1* haploinsufficiency ($dcr\text{-}1^{Q1147Xl+}$) replicated the nutrient-associated

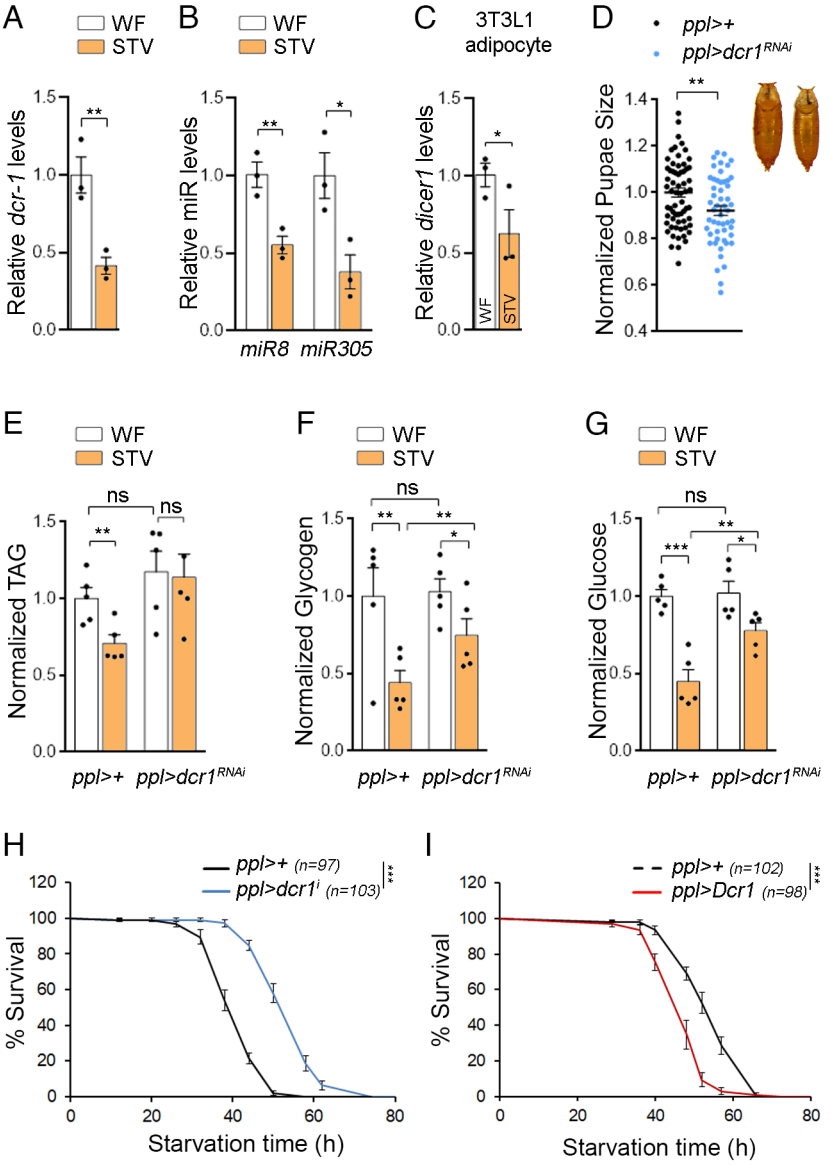

Fig. 1. Fat Body Dcr-1 Regulates Organismal Response to Challenging Nutrient Conditions. (*A*) qRT-PCR showing *dcr-1* mRNA levels in the FB of control (w^{1118}) animals subjected to well-fed (WF) or starved (STV) conditions. Results are expressed as fold induction with respect to WF. (*B*) qRT-PCR showing mature miRNA levels in the FB of control (w^{1118}) animals in WF or STV. (*C*) *dicer1* mRNA levels in 3T3L1 adipocytes exposed to 1 h of serum deprivation. (*D*) Relative pupal size of control (*ppl*>+) and *ppl*>*dcr-1*^{RNAi} animals raised in standard food. (*E–G*) Relative TAG (*E*), glycogen (*F*) and glucose (*G*) levels of control (*ppl*>+) and *ppl*>*dcr-1*^{RNAi} adult flies (males) maintained in WF or exposed to STV. Data were normalized to protein concentration and presented as a ratio with respect to control animals. (*H* and *I*) Survival rates to nutrient deprivation of adult flies (males) of the genotypes *ppl*>*dcr-1*^{RNAi} (*H*) or *ppl*>*Dcr1* (*I*) compared to control flies (*ppl*>+) subjected to the same procedure. See *SI Appendix*, Table S1 for n, p, median, and maximum survival values. Mean ± SEM. **P* < 0.05; ***P* < 0.01; ****P* < 0.001; ns: not significant. Genotypes: *ppl*>+ (*w*; ppl-GAL4/+); ppl*>*dcr-1*^{RNAi} (*w*; ppl-GAL4/+; UAS-dcr-1*^{RNAi}*/+); ppl*>*Dcr1* (*w*; ppl-GAL4/+; UAS- Dcr1/+).*

decline in miRNA expression [*SI Appendix*, Fig. S1; (3)]. The ratio of mature miRNAs to their respective precursor miRNAs (miR/pre-miR ratio) were also reduced in the FB of starved animals (*SI Appendix*, Fig. S1) strongly suggesting that miRNA processing is affected in these animals.

To better understand the role of adipose Dcr-1 in metabolic homeostasis and nutrient stress responses, we analyzed the impact of FB-specific depletion of Dcr-1 on animal size and energy resources, both under fed conditions and after nutrient deprivation. To reduce Dcr-1 levels in the FB, we expressed *dcr-1*^{RNAi} under the control of the FB-specific *ppl-Gal4* driver (referred to as *ppl>dcr1*^{RNAi}). While maintained on a normal diet, the *ppl>dcr1*^{RNAi} animals exhibited significant reduction in pupal size (Fig. 1*D*) and showed an important increase in size and number of lipid droplets (*SI Appendix*, Fig. S1). Under STV, *ppl>dcr1*^{RNAi} adult flies showed a reduction in the consumption rate of TAG, glycogen and glucose compared to control flies (Fig. 1 *E*–*G*). This reduction in mobilization of energy stores is likely due to increased levels of Dmp53 activity, which is negatively regulated by miR-305 in the FB of well-fed animals and has a proposed role in controlling systemic insulin signaling and reducing glycolysis in the FB (3, 12). Conversely, overexpressing Dcr-1 had the opposite effect and showed an accelerated consumption of energy stores under STV (*SI Appendix*, Fig. S1). We then evaluated the impact of Dcr-1 expression on survival rates of adult flies subjected to starvation conditions. Reducing Dcr-1 levels, either through heterozygous *dcr-1*$^{Q1147X/+}$ or *ppl>dcr1*^{RNAi} animals, increased the survival rates of adult flies during nutrient deprivation [Fig. 1*H* and *SI Appendix*, Fig. S1; (3)], while Dcr-1 overexpression in the FB reduced starvation resistance compared to control flies (Fig. 1*I*). This strongly suggests that Dcr-1 plays a critical role in regulating energetic homeostasis and organismal survival under nutrient deprivation. It is noteworthy that crosses of the *ppl-Gal4* driver to either the *w*^{1118} background (*ppl>+*) or control RNAi lines (UAS-GFP^{VALIUM10} and UAS-*white*^{RNAi}) exhibited similar survival rates upon fasting, as shown in *SI Appendix*, Fig. S1 and Table S1.

In cultured mammalian cells, Dicer1 expression has been shown to be affected by several stress conditions, including hypoxia, UV radiation, and oxidative stress (13–15). We then investigated the potential contribution of FB Dcr-1 to stress responses in *Drosophila*. Notably, when exposed to the oxidizing agent paraquat (PQ), animals showed a decrease in *dcr-1* transcript levels in the FB (Fig. 2*A*), and both *dcr-1*$^{Q1147X/+}$ and *ppl>dcr-1*^{RNAi} adult flies showed increased survival rates to PQ treatment compared to control flies exposed to the same treatment (Fig. 2 *C* and *D* and *SI Appendix*, Fig. S2). Additionally, the results of our study revealed a significant decline in *dcr-1* transcript levels in the abdomen of aging adult flies. The levels were found to be significantly lower in 30-day-old animals compared to their 10-d–old counterparts, as shown in Fig. 2*B*. We then compared the lifespan of *dcr-1* mutants and control animals using the *dcr-1*^{Q1147X} allele, backcrossed six times into the *w*^{1118} genetic background. Strikingly, heterozygous *dcr-1*^{Q1147X} mutant animals showed a remarkable increase in lifespan compared to control adult flies (Fig. 2*E* and *SI Appendix*, Table S1), making Dcr-1's role pivotal for future aging research. Moreover, FB-specific expression of *dcr-1*^{RNAi} showed similar lifespan extension (Fig. 2*F* and *SI Appendix*, Table S1) suggesting the effect of Dcr-1 on longevity can be partially explained by its role in the *Drosophila* adipose tissue. Overall, these results indicate a critical role for fat body Dcr-1 in regulating metabolism, stress resistance, and longevity in *Drosophila*.

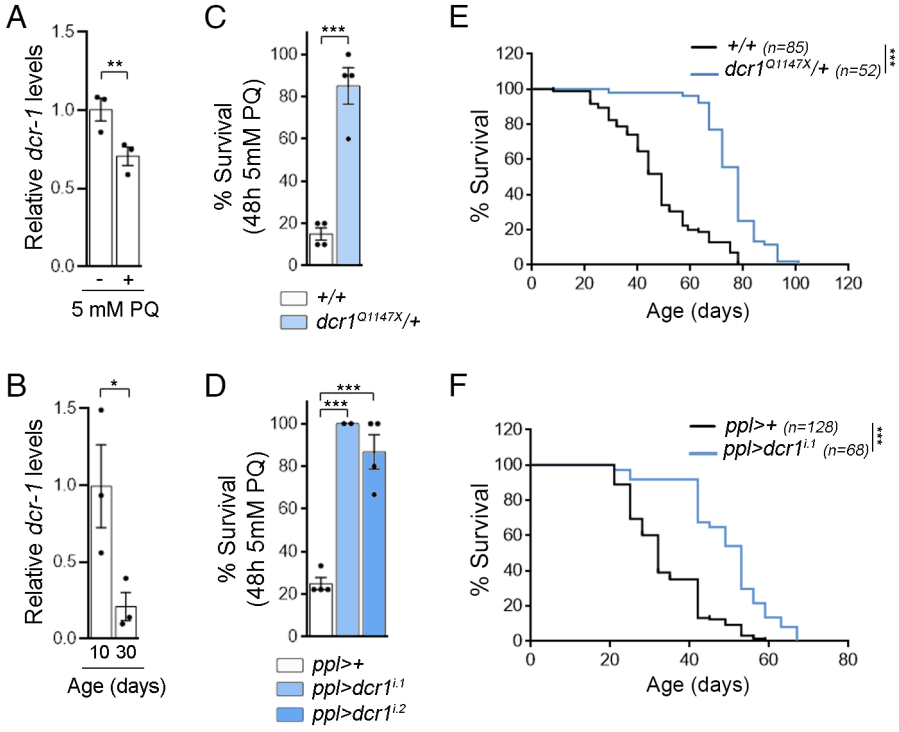

Fig. 2. Fat Body Dcr-1 Regulates Oxidative Stress Response and Longevity. (*A*) qRT-PCR showing *dcr-1* mRNA levels in the FB of control (*w*^{1118}) larvae in the presence of paraquat or vehicle. Results are expressed as fold induction with respect to control animals. (*B*) qRT-PCR showing *dcr-1* mRNA levels in the abdomen of 10- vs. 30-d–old adult flies. Results are expressed as fold induction with respect to 10-d–old animals. (*C* and *D*) Survival rates after 48 h paraquat treatment of adult flies (males) of the indicated genotypes compared to control flies subjected to the same procedure. (*E* and *F*) Lifespan extension (expressed as % survival) of adult flies (males) of the indicated genotypes maintained in regular food compared to control flies subjected to the same procedure. See *SI Appendix*, Table S1 for n, p, median, and maximum survival values. Mean ± SEM. **P* < 0.05; ***P* < 0.01; ****P* < 0.001; ns: not significant. Genotypes: *ppl>+ (w*; ppl-GAL4/+); ppl>dcr-1*^{RNAi} *(w*; ppl-GAL4/+; UAS-dcr-1*^{RNAi}*/+); +/+ (w*^{1118}*); dcr1*^{Q1147X}*/+ (w*^{1118}*; dcr1*^{Q1147X}*/+).*

JNK-FOXO Signaling Regulates Dcr-1 Expression under Starvation Conditions. The transcription factors (TFs) FOXO and REPTOR/REPTOR-BP are activated under STV and have been found to mediate transcriptional changes related to nutrient deprivation in *Drosophila* (16, 17). This raises the possibility that the levels of *dcr-1* may be directly regulated by either of these TFs. To test this hypothesis, we measured *dcr-1* transcript levels in the FB of starved animals that expressed either $foxo^{RNAi}$ or $reptor^{RNAi}$ controlled by FB-specific *Gal4* drivers. Interestingly, the reduced *dcr-1* transcript levels observed in the FB after 24 h of STV treatment were reversed both by $foxo^{RNAi}$ expression and in heterozygous $foxo^{25/D94}$ animals (Fig. 3*A* and *SI Appendix*, Fig. S3). Furthermore, FB-specific overexpression of a constitutively active FOXO (18) using either ppl-Gal4 (larval FB) or yolk-Gal4 (expressed only in the fat body of adult females) was sufficient to reduce *dcr-1* transcript levels in well-fed conditions (Fig. 3*B* and *SI Appendix*, Fig. S3). However, no differences were observed in *dcr-1* transcript levels when expressing $reptor^{RNAi}$, supporting a distinct role for FOXO in the regulation of *dcr-1* transcriptional levels in this context (*SI Appendix*, Fig. S3).

To determine whether the reduction of Dcr-1 expression mediated by FOXO has an impact on miRNA biogenesis and/or activity, we used a miRNA activity reporter (miR-GFP) that consisted of the wild-type *dMyc 3′ UTR* cloned into a *tubulin*-promoter-EGFP reporter plasmid (19). This reporter showed an increase in GFP expression levels either when Dcr-1 was depleted or upon STV treatment (*SI Appendix*, Fig. S4). Interestingly, while STV treatment increased miR-GFP levels in FB control cells, GFP levels in $foxo^{RNAi}$-expressing cells remained low (Fig. 3*C*; compare GFP levels in control (RFP^-) and $foxo^{RNAi}$ (RFP^+) expressing cells). Consistent with a role of FOXO in regulating miRNA biogenesis, the expression of FOXO in single FB cells increased GFP levels of the miR-sensor in well-fed animals (Fig. 3*C*). Conversely, STV-induced expression of the miR-GFP sensor was not affected in cells expressing $reptor^{RNAi}$ (Fig. 3*C*). To examine the possibility of FOXO directly regulating *dcr-1* transcription, we first evaluated the presence of potential FOXO DNA binding sites in *dcr-1* gene locus (20, 21). Using FIMO (22), we identified two canonical FOXO binding sites located 120 bp (BS_1: TTTTGTTGATA; *P* value= 2.7e-4) and 1,900 bp (BS_2: TTTTGTTTACA; *P* value= 1.81e-5) upstream the transcription start site (*SI Appendix*, Fig. S3). Chromatin immunoprecipitation followed by qPCR analysis (ChIP-qPCR) confirmed in vivo FOXO binding to these specific sites located in *dcr-1* promoter. As shown in Fig. 3*E*, ChIP-qPCR experiments revealed that FOXO binds to the predicted *dcr-1* sites with similar affinity to its well-known target gene *4ebp*. We confirmed these results by analyzing FOXO ChIP-seq datasets from whole L3 *Drosophila* larvae (doi:10.17989/ENCSR548EHZ; *SI Appendix*, Fig. S3). These results suggest that FOXO activation during nutrient deprivation negatively regulates *dcr-1* transcription through conserved FOXO DNA-binding sites in its promoter region.

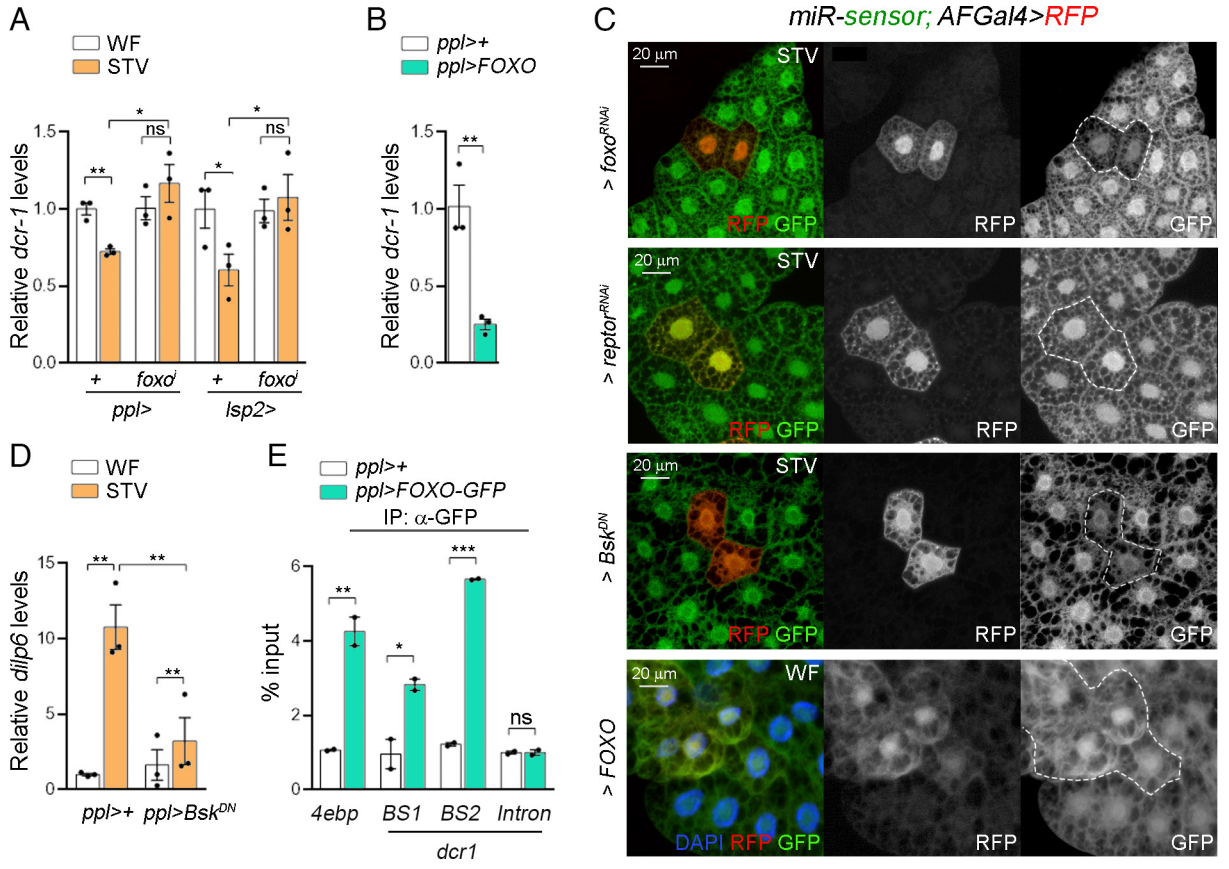

Fig. 3. FOXO Regulates Dcr-1 Expression and miRNA Biogenesis in the FB of Starved Animals. (*A* and *B*) qRT-PCR showing *dcr-1* mRNA levels in the FB of larvae expressing the indicated transgenes under ppl-Gal4 (*A* and *B*) or lsp2-Gal4 (*A*) maintained in WF conditions or subjected to STV. Results are expressed as fold induction with respect to control animals. (*C*) FB cells labeled to visualize a miR-GFP sensor (miR-sensor; in green or white) from WF or STV larvae expressing the indicated transgenes (marked by the expression of RFP, in red). (*D*) *dilp6* mRNA levels in the FB of control (*ppl>+*) or Bsk^{DN} expressing larvae (*ppl>*Bsk^{DN}) under WF or STV conditions. (*E*) ChIP-qPCR assays showing the binding of FOXO-GFP to the *dcr-1* (BS1 and BS2) and *4ebp* promoters in the FB of *ppl>FOXO-GFP* larvae. Dcr-1 intronic region is being used as a negative control. Mean ± SEM. *$P < 0.05$; **$P < 0.01$; ***$P < 0.001$; ns: not significant. Genotypes: *ppl>+ (w*; ppl-GAL4/+); ppl>*$foxo^{RNAi}$ *(w*; ppl-GAL4/+; UAS-* $foxo^{RNAi}$*/+); ppl>FOXO (w*; ppl-GAL4/+; UAS-FOXO/+); ppl>*bsk^{DN} *(w*; ppl-GAL4/+; UAS-* bsk^{DN}*/+); ppl>FOXO-GFP (w*; ppl-GAL4/+; UAS-FOXO:GFP/+); miR-sensor:AFGal4>RFP (yw,hsFlp; miR-sensor/+; Act5C(FRT.CD2)-Gal4, UAS-RFP); lsp2>+ (*y^1,w^{1118}*; lsp2-GAL4/+); lsp2>*$foxo^{RNAi}$ *(*y^1,w^{1118}*; lsp2-GAL4/UAS-*$foxo^{RNAi}$*).*

FOXO has previously been shown to be regulated by the JNK pathway (23). To determine whether JNK is acting upstream of FOXO in the FB under nutrient stress conditions, we measured *dilp6* and *4ebp* transcript levels, well-described transcriptional targets of FOXO in *Drosophila*. The starvation treatment of midL3 larvae led to a significant increase in *dilp6* and *4ebp* expression in the FB, an effect significantly inhibited upon expression of a dominant-negative form of Basket (*ppl>Bsk^{DN}*) (Fig. 3*D* and *SI Appendix*, Fig. S3). Consistently with JNK acting upstream of FOXO, the induction of miR-GFP sensor was impaired in FB cells of starved animals lacking JNK signaling by expression of Bsk^{DN} (Fig. 3*C*; compare GFP levels in control (RFP$^-$) and *Bsk^{DN}* (RFP$^+$) expressing cells). Similarly, the reduction of *dcr-1* levels upon nutrient deprivation was reverted by expression of Bsk^{DN} (*SI Appendix*, Fig. S3). These results indicate that FOXO acts in the FB upon nutrient deprivation to repress Dcr-1 expression and miRNA biogenesis downstream of JNK signaling.

FOXO-Dependent Regulation of Dcr-1 Expression Contributes to Starvation Resistance. We then evaluated whether FOXO-mediated *dcr-1* repression is required for survival rates under nutrient deprivation. As previously demonstrated, both *foxo* mutant animals [*foxo$^{21/25}$* (24)] and animals expressing *foxo^{RNAi}* in the FB (*ppl>foxo^{RNAi}*) showed reduced survival rates to STV conditions compared to control flies (Fig. 4*A*, *SI Appendix*, Fig. S5 and *SI Appendix*, Table S1). Interestingly, the STV sensitivity caused by FOXO depletion was reversed upon coexpression of *dcr-1^{RNAi}* in the FB (*ppl>foxo^{RNAi}, dcr-1^{RNAi}*flies; Fig. 4*C*; *SI Appendix*, Table S1), consistent with FOXO's role in repressing *dcr-1*. Furthermore, the increased survival rates caused by FOXO overexpression were also reversed by Dcr-1 expression (*Cg^{ts}>FOXO, Dcr-1* flies; Fig. 4*B* and *SI Appendix*, Table S1).

Among the miRNAs expressed in the adipose tissue, miR-305 appears to be particularly responsive to changes in nutrient and Dcr-1 levels (Fig. 1*B*, *SI Appendix*, Fig. S1 and ref. 3). Interestingly, the *Drosophila* ortholog of mammalian p53 (Dmp53) has been previously shown to be repressed by miR-305 in the FB of well-fed animals. Under nutrient deprivation, however, reduced Dcr-1 levels impairs miRNA processing thus alleviating miR-305-repression of Dmp53, which has been established as essential for metabolic homeostasis and stress resistance (3, 12). In fact, the expression of the dominant negative Dmp53$^{H159.N}$ reversed the increased survival rates caused by *dcr-1^{RNAi}* expression in the FB of starved adult flies (3). The question then arose as to whether increased miR-305 levels in FOXO-depleted animals could explain their reduced survival rates under nutrient deprivation. To address this question, we used a miR-305 sponge transgene (miR-305^{SP}), which has been previously established as impairing miR-305 function (25–27). This was demonstrated by a rise in *dmp53* transcript levels (*SI Appendix*, Fig. S5), a known miR-305 target gene (3), upon miR-305^{SP} expression in the FB. Strikingly, FB-specific expression of miR-305^{SP} completely reversed the STV sensitivity caused by FOXO depletion (*ppl>foxo^{RNAi}, miR-305^{SP}* flies; Fig. 4*D*; *SI Appendix*, Table S1). These results indicate that FOXO activity in the FB of starved animals reduces *dcr-1* levels, thus affecting miRNA biogenesis and starvation resistance.

Discussion

The expression levels of Dcr-1 have been shown to be regulated in response to various metabolic stimuli, such as changes in oxygen levels or nutrient availability (3, 13, 14). In addition, Dcr-1 interacts with key players in key nutrient-sensing pathways such as mammalian target of rapamycin (mTOR) and AMP-activated

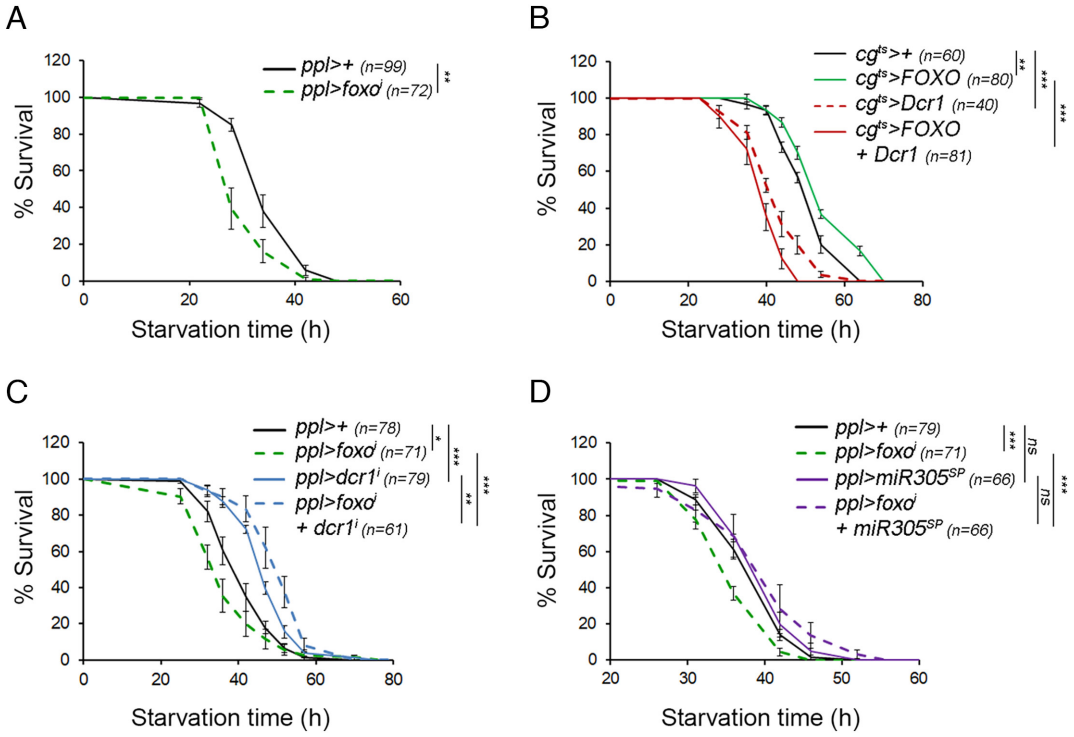

Fig. 4. Starvation Resistance upon FB-Specific Depletion of FOXO and the miRNA Machinery. (*A–D*) Survival rates to nutrient deprivation of adult flies (males) of the indicated genotypes compared to control flies subjected to the same procedure. See *SI Appendix*, Table S1 for n, p, median, and maximum survival values. Genotypes: *ppl>+ (w*; ppl-GAL4/+); ppl>dcr-1^{RNAi} (w*; ppl-GAL4/+; UAS-dcr-1^{RNAi}/+); ppl>foxo^{RNAi} (w*; ppl-GAL4/+; UAS- foxo^{RNAi}/+); ppl> foxo^{RNAi} + dcr-1^{RNAi} (w*; ppl-GAL4/+; UAS-dcr-1^{RNAi}/UAS-foxo^{RNAi}); ppl>miR305^{SP} (w*; ppl-GAL4/+; UAS-miR305^{SP}/+); ppl>foxo^{RNAi} + miR305^{SP} (w*; ppl-GAL4/+; UAS-miR305^{SP}/UAS- foxo^{RNAi}); cg^{ts}>+ (y^{1},w^{1118}; cg-GAL4/+; tub-Gal80^{ts}/+); cg^{ts}>FOXO (y^{1},w^{1118}; cg^{ts}-GAL4/UAS-FOXO; tub-Gal80^{ts}/+); cg^{ts}>Dcr1 (y^{1},w^{1118}; cg-GAL4/+; tub-Gal80^{ts}/UAS-Dcr1); cg^{ts}>FOXO + Dcr1 (y^{1},w^{1118}; cg^{ts}-GAL4/UAS-FOXO; tub-Gal80^{ts}/UAS-Dcr1).*

protein kinase (AMPK), leading to the modulation of energy metabolism (3, 15). Dicer1 depletion is frequently observed in human cancer and has been shown to enhance tumor development (28–31). This highlights the important role that Dcr-1 plays in allowing cells to sense and respond to environmental stress, which is crucial in disease development and aging. In the present study, we reveal a critical role for Dcr-1 in regulating metabolism, stress resistance and longevity in *Drosophila.* As reported in mammals, *dcr-1* expression in the *Drosophila* adipose tissue is regulated by several stress and physiological conditions such as aging, oxidative stress and nutrient deprivation. Reducing Dcr-1 levels and miRNA processing leads to altered glucose and energy homeostasis and increased viability in response to starvation conditions and oxidative stress. Studies in mice preadipocytes have also shown that Dicer1 is regulated under stress conditions (5). However, adipose-specific *dicer1* knockout mice (adipose-Dicer^{KO}) showed increased sensitivity to injected PQ compared to control animals (5). These conflicting results may be due to premature aging in adipose-Dicer^{KO} mice, characterized by increased senescent markers in both adipose and nonadipose tissue, which could affect the animals' response to acute stress stimuli (5). Moreover, Dcr-1-depleted flies showed dramatic increases in the size and number of LDs (*SI Appendix*, Fig. S1), and emerging evidence indicates that LDs can provide protection against oxidative stress (32). The extent to which Dcr-1's protective effect against PQ is related to lipid metabolism regulation remains to be determined. It further remains unclear the reason why the decline in Dcr-1 levels in aging flies does not result in increased resistance to oxidative stress (33). Aging is characterized by the progressive decline of multiple cellular processes and homeostatic mechanisms, and numerous miRNAs that are differentially expressed during aging have been described (34, 35). Thus either miRNAs or miRNA-target genes involved in promoting stress tolerance in young animals might not be expressed in old animals.

FOXO transcription factors have long been recognized as key regulators of stress responses and aging (36). *Drosophila* expresses a single FOXO gene that is involved in crucial biological processes, such as metabolic homeostasis, redox balance, stress response, and animal lifespan (37, 38). In this work, we show that JNK-dependent activation of FOXO in the fat body of starved animals represses Dcr-1 expression, which, in turn, leads to reduced miRNA biogenesis. FOXO-mediated *Dcr-1* repression is necessary for regulating Dmp53 and promoting organismal survival during nutrient deprivation. The fact that FOXO binds to canonical DNA binding sites located in *dcr-1* locus strongly suggests direct transcriptional regulation. These results provide mechanistic insights and highlight the essential role of the JNK-FOXO pathway integrating nutrient availability with miRNA biogenesis in the *Drosophila* fat body. Interestingly, FOXO has previously been shown to regulate small interfering RNA (siRNA) biogenesis by directly regulating the expression of genes involved in the siRNA pathway, including Argonaute-2 (AGO2) and Dicer-2, thereby increasing the efficiency of siRNA silencing (39). FOXO overexpression has also been shown to increase expression of AGO1 (39), an essential component of the miRNA machinery, though the physiological relevance of this regulation remains uncertain. In contrast, our results indicate that FOXO directly represses *dcr-1* expression in the adipose tissue of flies subjected to nutrient deprivation. Therefore, the modulation of small RNA pathways by FOXO activity may occur in a cell type and context-dependent manner. In flies, FOXO activation mediates lifespan extension caused by reduced insulin/insulin-like growth factor-like signaling (IIS) (40), and tissue-specific activation of FOXO is sufficient to extend lifespan (10, 11, 41). Interestingly, *dcr-1* levels are reduced in aged adult flies and *dcr-1* heterozygous animals exhibit a dramatic extension in lifespan. Whether *dcr-1* repression is required for FOXO-mediated lifespan extension remains to be determined.

It has previously been proposed that Dicer1 activity contributes to the aging process. In mice, *dicer1* deficiency accelerates age-associated phenotypes and mitigates the positive effects of dietary restriction (42). In *C. elegans*, worms overexpressing Dcr-1 in the intestine are stress resistant while whole body *dcr-1* loss-of-function mutations produce short-lived animals (5). *Dcr-1* homozygous mutants are embryonic lethal in *Drosophila* (43, 44); however, *dcr-1* heterozygous adult flies showed a dramatic lifespan extension and are resistant to both starvation and oxidative stress. It is important to note that halving the dose of *dcr-1* has a subtle impact on miRNA biogenesis, with a reduction of 20 to 30% in mature miRNA levels, indicating that small changes in specific miRNA levels can have significant effects on animal physiology. Interestingly, enoxacin treatment, a drug that interferes with miRNA biogenesis, extends lifespan and promotes survival under oxidative stress conditions in *C. elegans* (45). These results point to an important role of Dcr1 in regulating longevity and stress resistance and suggest that different levels of Dcr-1 may account for discrepancies in phenotypes observed when reducing or eliminating this gene.

The activation of *Drosophila* p53 (Dmp53) in the FB has been linked to the regulation of adaptive physiological responses to low nutrient availability by remotely controlling insulin secretion and autophagy (3, 12). A dual mechanism has been proposed to regulate Dmp53 activity under nutrient stress. Firstly, repression of *dcr-1* following starvation treatments contributes to Dmp53 activation by alleviating the targeting of Dmp53 by miR-305 in the FB (3). Secondly, AMPK-dependent activation of Dmp53 upon starvation is required for metabolic and physiological changes that promote organismal resistance to nutrient deprivation (12). The fact that FOXO (through *dcr-1* repression) and AMPK, two key players in the response to energy and nutrient stress, are required for the Dmp53 activation emphasizes the essential role this transcription factor plays in the adipose tissue as part of a nutrient sensing mechanism that orchestrates metabolic adaptation to challenging nutrient conditions. Our results therefore place FOXO in a crucial position connecting nutrient sensing to *dcr-1* expression and miRNA biogenesis. Further research is required to determine whether *dcr-1* is itself regulated by miRNAs in *Drosophila,* as has been described in vertebrates (46, 47). A miRNA/Dcr-1 autoregulatory loop could be important for dynamic responses to nutrient availability, involving changes in Dcr-1 levels and specific miRNA-target genes that regulate cell and tissue homeostasis.

Materials and Methods

***Drosophila* Strains and Maintenance.** The following *Drosophila* strains were used: w^{1118}, ppl-Gal4 (BDSC:58768), lsp2-Gal4 (BDSC:6357), cg-Gal4 (BDSC:7011); UAS-dcr-1^{RNAi} (VDRC11429); UAS-*dcr-1*^{RNAi} (BDSC:34826); UAS-FOXO-GFP (Gift from Pablo Wappner); UAS-foxo^{RNAi} (BDSC:27656); UAS-FOXO (18); UAS-reptor^{RNAi} (BDSC:25983); Myc$^{3'UTR}$-sensor (19); dcr-1^{Q1147X} (48); foxo^{21} (18); foxo^{25} (18); foxo$^{\Delta 94}$ (49); hsFLP; act>y+>Gal4,UAS-RFP (3); yolk-Gal4 (BDSC:58814); UAS-Dcr1 (BDSC:36510); UAS-mir-305^{SP} (BDSC:61423); UAS-Bsk^{K53R} (UAS-bsk^{DN} in the text; BDSC:9311); UAS-GFP^{VALIUM10} (BDSC:35786); UAS-white^{RNAi} (BDSC:33762). Genotypes are detailed in *SI Appendix*, Table S2. Flies were reared at 25 °C on standard media containing: 4% glucose, 40 g/L powder yeast, 1% agar, 25 g/L wheat flour, 25 g/L cornflour, 4 mL/L propionic acid and 1.1 g/L nipagin.

Fly Husbandry and Mosaic Analysis. Gal4/UAS binary system was used to drive transgene expression in the different *Drosophila* tissues (50) and experimental crosses were performed at 25 °C, unless otherwise specified. Females of the GAL4 lines were crossed to males of the corresponding UAS line(s), and

the larval or adult progeny were analyzed; only males from the F1 were used for phenotypic analysis in adults. Crossing Gal4 driver lines to the w^{1118} background, UAS-GFP^{VALIUM10} or UAS-*white*^{RNAi} provided controls for each experiment.

Flp/Out system was used to generate RFP-marked clones. Flies from *hsFLP; act>y+>Gal4, UAS-RFP* were crossed to corresponding UAS-transgene lines at 25 °C and spontaneous recombination events taking place in the fat body prior to the onset of endoreplication were analyzed (51).

Starvation Treatments, Survival Experiments, and Lifespan. For starvation treatments in larvae, eggs were collected for 4-h intervals, and larvae were transferred to vials containing standard food immediately after hatching (first instar larvae, L1) at a density of 50 larvae per tube. Larvae were then raised at 25 °C for 72 h prior to the starvation assay. Mid-third instar larvae were washed with PBS and placed in inverted 60-mm petri dishes with phosphate-buffered saline (PBS) soaked Whatman paper (starvation, STV) or maintained in standard food (well fed, WF). Each plate was sealed with Parafilm and incubated at 25 °C for the duration of the experiment. After the starvation period, full larvae or dissected fat bodies were used for immunostaining, RNA extraction, and metabolite measurements. For paraquat treatments in larvae, 50 mid-L3 larvae were placed in tubes containing food plus 25 mg/mL of paraquat (Sigma) or an equivalent volume of MilliQ water as a control. After 6 h, dissected fat bodies were used for RNA extraction. For starvation sensitivity assays, 5- to 7-d–old flies (males) of each genotype were transferred into vials containing 0.5% agar in PBS (10 flies per vial). Flies were transferred to new tubes every day, and dead flies were counted every 6 h. For each experimental condition, a minimum of six replicates were used to calculate the mean (and SEM) percentage of viable flies per time point. Control animals were always analyzed in parallel in each experimental condition. For paraquat treatments, adults were transferred to food containing 2,5 mg/mL of paraquat (Sigma) or an equivalent volume of MilliQ water as a control. For lifespan experiments, 5- to 7-d–old flies of each genotype were transferred into vials containing standard food. Flies were transferred to new tubes every day, and dead flies were counted. Statistics were performed using GraphPad Prism 6.0 software as described below. Number of individuals used in each experiment is detailed in *SI Appendix*, Table S1.

Immunostainings. Mid-third instar larvae were dissected in cold PBS and fixed in 4% formaldehyde/PBS for 20 min at room temperature. They were then washed and permeabilized in PBT (0.2% Triton X-100 in PBS) for 30 min and blocked in BBT (0.3% BSA, 250 mM NaCl in PBT) for 1 h. Samples were incubated overnight at 4 °C with primary antibody diluted in BBT, washed three times (15 min each) in BBT and incubated with secondary antibodies for 1.5 h at room temperature. After three washes with PBT (15 min each), dissected tissues were placed in a mounting medium (80% glycerol/PBS containing 0.05% n-propyl-gallate). Images were acquired on a Leica SP8 inverted confocal microscope and analyzed and processed using Fiji (52) and Adobe Photoshop. The following primary antibodies were used: mouse anti-GFP (12A6, DSHB). The following secondary antibodies were used: anti-mouse IgG-Alexa Fluor 488 (Jackson InmunoResearch).

For BODIPY staining, five mid-third instar larvae were dissected in cold PBS and incubated 5 min with BODIPY (ThermoFisher) at a final concentration of 0,5 uM in PBS. After washing, dissected tissues were placed in mounting medium (80% glycerol/PBS containing 0.05% n-propyl-gallate) and immediately imaged.

RNA Isolation and Quantitative RT-PCR. To measure mRNA levels, total RNA was extracted from cultured 3T3 L1 adipocytes, adult flies, whole larvae, or dissected FBs of 30 animals using TRIzol RNA Isolation Reagent (Invitrogen). First strand cDNA synthesis was performed using an oligo(dT)18 primer and RevertAid reverse transcriptase (ThermoFisher) under standard conditions. Quantitative PCR was performed on an aliquot of the cDNA with specific primers (*SI Appendix*, Table S2) using the StepOnePlus Real-Time PCR System. Expression values were normalized to *actin* transcript levels. Data were then normalized to control WF animals using the ΔΔ-CT, and fold change was calculated afterwards. In all cases, three independent samples were collected from each condition and genotype. Student's t test was used for statistical analysis. In the case of pre-miRNAs, first-strand cDNA synthesis was performed using random hexamers. To quantify mature miRNA levels, we followed a two-step process (53): 1) RT with a miRNA-specific stem loop primer (*SI Appendix*, Table S2) followed by 2) quantitative PCR using both a miRNA-specific forward primer and a universal reverse primer (*SI Appendix*, Table S2).

Chromatin Immunoprecipitation. Immunoprecipitation assay was performed with a specific anti-GFP antibody (12A6, DSHB) on L3 control larvae (*ppl>+*) and FOXO overexpressing larvae (*ppl>FOXO-GFP*) following the modEncode protocol (54). The specific immunoprecipitated DNA was detected by quantitative PCR using primers listed in *SI Appendix*, Table S2.

Metabolic Assays. TAG, glycogen, and glucose levels were determined as previously described (12). Briefly, 5 to 7-d–old adult flies were fast frozen in liquid nitrogen, homogenized in 200 µL of PBS, and immediately incubated at 70 °C for 10 min to inactivate endogenous enzymes. For quantification of glucose, hemolymph from 15 larvae was diluted 1:100 and incubated at 70 °C for 5 min. TAG levels were determined using a serum triglyceride determination kit (Sigma, TR0100) according to the manufacturer's protocol. For glycogen measurements, 40 µL of heat-treated homogenates were incubated with or without 1 unit of amyloglucosidase (Sigma, A7420) for 2 h at 55 °C and assayed using a Glucose (GO) Assay Kit (Sigma, GAGO-20). Glycogen amounts were determined by subtracting from the total amount of glucose present in the sample treated with amyloglucosidase the amount of free glucose of untreated samples. Metabolite levels were normalized to protein concentration (BioRad Protein Assay). Five replicates for each genotype and condition were performed, and data were represented as a percentage of the corresponding levels in fed condition for each genotype.

Pupal Size. For pupal size measurements, eggs were collected for a 4-h interval and first instar larvae were transferred to new vials containing standard food immediately after eclosion at a density of 50 larvae per tube. Larvae were then raised at 25 °C until pupariation. Pupal volume was calculated by the formula $4/3\pi(L/2)(l/2)^2$ (L, length; l, diameter). Images were taken with a Leica MZ10F Stereoscope, and measures were done using ImageJ software. Pupal size values were shown as the ratio with respect to control animals.

Mice 3T3L1 Culture Cells. Differentiation of mice 3T3-L1 cells (ATCC® CL-173TM) was performed as suggested by ATCC. Briefly, cells were grown in complete medium [DMEM (Sigma) supplemented with 10% fetal bovine serum (Natocor) and 1% antibiotics (Pen/Strep, Sigma)] until the culture reached 100% confluence. Cells were incubated as a confluent culture for another 48 h, and medium was replaced with differentiation medium containing 1.0 µM dexamethasone, 0.5 mM methylisobutylxanthine (IBMX), and 1.0 µg/mL insulin. After 48 h, differentiation medium was replaced with complete medium containing 1.0 µg/mL Insulin and at 72 h later, the medium was replaced by complete medium. Cells were fully differentiated 7 d after induction, as evidenced by observation of lipid droplet formation. For the starvation treatment, fully differentiated cells were serum deprived for the indicated time and cells were harvested for RNA extraction.

Quantification and Statistical Analysis. For starvation, sensitivity assays and lifespan experiments statistics were performed using GraphPad Prism6, which uses the Kaplan–Meier estimator to calculate survival fractions as well as median and maximum survival values. Curves were compared using the log-rank (Mantel–Cox) test. The two-tailed *P* value indicates the value of the difference between the two entire survival distributions at comparison.

GraphPad Prism6 was used for statistical analysis and graphical representations based on three or more replicates for each experiment. All significance tests were carried out with unpaired two tailed Student's *t* tests. Significance *p* values: $^{*}P < 0.05$, $^{**}P < 0.01$, $^{***}P < 0.001$, $^{****}P < 0.0001$, $^{ns}P > 0.05$.

Images were acquired on a Leica SP8 inverted confocal microscope and analyzed and processed using Fiji (52) and Adobe Photoshop. Tissue orientation and/or position was adjusted in the field of view for images presented. No relevant information was affected.

Data, Materials, and Software Availability. All study data are included in the article and/or *SI Appendix*.

ACKNOWLEDGMENTS. We thank Pablo Wappner, Andres Garelli, Marco Milan, Patrick Jouandin, Vienna Drosophila RNAi Center, Drosophila Bloomington Stock Center, and the Developmental Studies Hybridoma Bank for flies and antibodies. M.C.I, J.A.S and M.P.G. are funded by PhD fellowships from the Consejo Nacional de Investigaciones Científicas y Técnicas. M.G.T., G.L.B., and A.D. are members of the Consejo Nacional de Investigaciones Científicas y Técnicas; G.L.B. is Professor at the University of Buenos Aires. A.D. is Professor at Universidad Nacional del Litoral (UNL). This work was supported by grants from the Agencia Nacional de Promoción Científica y Tecnológica, Argentina and UNL.

1. G. S. Heyn, L. H. Corrêa, K. G. Magalhães, The Impact of Adipose Tissue-Derived miRNAs in Metabolic Syndrome, Obesity, and Cancer. *Front. Endocrinol.* **(Lausanne). 11**, 563816. (2020).
2. L. Kappeler, Role of Adipose Tissue microRNAs in the Onset of Metabolic Diseases and Implications in the Context of the DOHaD. *Cells* **11** (2022).
3. L. Barrio, A. Dekanty, M. Milán, MicroRNA-Mediated Regulation of Dp53 in the Drosophila Fat Body Contributes to Metabolic Adaptation to Nutrient Deprivation. *Cell Rep.* **8**, 528–541 (2014).
4. M. Oliverio *et al.*, Dicer1-miR-328-Bace1 signalling controls brown adipose tissue differentiation and function. *Nat. Cell Biol.* **18**, 328–336 (2016).
5. M. A. Mori *et al.*, Role of microRNA processing in adipose tissue in stress defense and longevity. *Cell Metab.* **16**, 336–347 (2012).
6. M. A. Mori *et al.*, Altered miRNA processing disrupts brown/white adipocyte determination and associates with lipodystrophy. *J. Clin. Invest.* **124**, 3339–3351 (2014).
7. B. B. Brandão *et al.*, Dynamic changes in DICER levels in adipose tissue control metabolic adaptations to exercise. *Proc. Natl. Acad. Sci. U. S. A.* **117**, 23932–23941 (2020).
8. E. Parra-Peralbo, A. Talamillo, R. Barrio, Origin and Development of the Adipose Tissue, a Key Organ in Physiology and Disease. *Front. cell Dev. Biol.* **9** (2021).
9. E. L. Arrese, J. L. Soulages, Insect fat body: energy, metabolism, and regulation. *Annu. Rev. Entomol.* **55**, 207–225 (2010).
10. M. E. Giannakou *et al.*, *Long-Lived Drosophila with Over- expressed dFOXO in Adult Fat Body.* **305**, 2004 (2004).
11. D. S. Hwangbo, B. Gersham, M. Tu, M. Palmer, *Drosophila dFOXO controls lifespan and regulates insulin signalling in brain and fat body.* **429**, 562–567 (2004).
12. M. C. Ingaramo, J. A. Sánchez, N. Perrimon, A. Dekanty, Fat Body p53 Regulates Systemic Insulin Signaling and Autophagy under Nutrient Stress via Drosophila Upd2 Repression. *Cell Rep.* **33** (2020).
13. D. Gibbings *et al.*, Selective autophagy degrades DICER and AGO2 and regulates miRNA activity. *Nat. Cell Biol.* **14**, 1314–21 (2012).
14. J. J. D. Ho *et al.*, Functional Importance of Dicer Protein in the Adaptive Cellular Response to Hypoxia. *J. Biol. Chem.* **287**, 29003–29020 (2012).
15. G. Blandino *et al.*, Metformin elicits anticancer effects through the sequential modulation of DICER and c-MYC. *Nat. Commun.* **3**, 865 (2012).
16. A. a Teleman, V. Hietakangas, A. C. Sayadian, S. M. Cohen, Nutritional control of protein biosynthetic capacity by insulin via Myc in Drosophila. *Cell Metab.* **7**, 21–32 (2008).
17. M. Tiebe *et al.*, REPTOR and REPTOR-BP Regulate Organismal Metabolism and Transcription Downstream of TORC1. *Dev. Cell* **33**, 272–284 (2015).
18. M. A. Jünger *et al.*, The Drosophila Forkhead transcription factor FOXO mediates the reduction in cell number associated with reduced insulin signaling. *J. Biol.* **2**, 20 (2003).
19. A. Ferreira, L. Boulan, L. Perez, M. Milán, Mei-P26 mediates tissue-specific responses to the brat tumor suppressor and the dMyc Proto-Oncogene in Drosophila. *Genetics* **198**, 249–258 (2014).
20. A. Birnbaum, X. Wu, M. Tatar, N. Liu, H. Bai, Age-dependent changes in transcription factor FoxO targeting in female Drosophila. *Front. Genet.* **10**, 312 (2019).
21. J. A. Castro-Mondragon *et al.*, JASPAR 2022: the 9th release of the open-access database of transcription factor binding profiles. *Nucleic Acids Res.* **50**, D165–D173 (2022).
22. C. E. Grant, T. L. Bailey, W. S. Noble, FIMO: scanning for occurrences of a given motif. *Bioinformatics* **27**, 1017–1018 (2011).
23. M. C. Wang *et al.*, *JNK Extends Life Span and Limits Growth by Antagonizing Cellular and Organism-Wide Responses to Insulin Signaling.* **121**, 115–125 (2005).
24. J. M. Kramer, J. D. Slade, B. E. Staveley, foxo is required for resistance to amino acid starvation in Drosophila. *Genome* **51**, 668–672 (2008).
25. M. Ueda, T. Sato, Y. Ohkawa, Y. H. Inoue, Identification of miR-305, a microRNA that promotes aging, and its target mRNAs in Drosophila. *Genes to Cells* **23**, 80–93 (2018).
26. T. A. Fulga *et al.*, A transgenic resource for conditional competitive inhibition of conserved Drosophila microRNAs. *Nat. Commun.* **61** (6), 1–10 (2015, 2015,).
27. D. Foronda, R. Weng, P. Verma, Y. W. Chen, S. M. Cohen, Coordination of insulin and notch pathway activities by microRNA miR-305 mediates adaptive homeostasis in the intestinal stem cells of the Drosophila gut. *Genes Dev.* **28**, 2421–2431 (2014).
28. A. Heravi-Moussavi *et al.*, Recurrent somatic DICER1 mutations in nonepithelial ovarian cancers. *N. Engl. J. Med.* **366**, 234–242 (2012).
29. M. S. Kumar, J. Lu, K. L. Mercer, T. R. Golub, T. Jacks, Impaired microRNA processing enhances cellular transformation and tumorigenesis. *Nat. Genet.* **39**, 673–677 (2007).
30. M. S. Kumar *et al.*, Dicer1 functions as a haploinsufficient tumor suppressor. *Genes Dev.* **23**, 2700–2704 (2009).
31. A. Ravi *et al.*, Proliferation and tumorigenesis of a murine sarcoma cell line in the absence of DICER1. *Cancer Cell* **21**, 848–855 (2012).
32. A. P. Bailey *et al.*, Antioxidant Role for Lipid Droplets in a Stem Cell Niche of Drosophila. *Cell* **163**, 340–353 (2015).
33. A. A. Belyi *et al.*, The resistance of Drosophila melanogaster to oxidative, genotoxic, proteotoxic, osmotic stress, infection, and starvation depends on age according to the stress factor. *Antioxidants* **9**, 1–18 (2020).
34. N. Noren Hooten *et al.*, Age-related changes in microRNA levels in serum. *Aging (Albany. NY)* **5**, 725–740 (2013).
35. A. De Lencastre *et al.*, MicroRNAs both promote and antagonize longevity in C. elegans. *Curr. Biol.* **20**, 2159–2168 (2010).
36. R. Martins, G. J. Lithgow, W. Link, Long live FOXO: Unraveling the role of FOXO proteins in aging and longevity. *Aging Cell* **15**, 196–207 (2016).
37. L. Partridge, J. C. Brüning, Forkhead transcription factors and ageing. *Oncogene* **27**, 2351–2363 (2008).
38. D. A. Salih, A. Brunet, FoxO transcription factors in the maintenance of cellular homeostasis during aging. *Curr. Opin. Cell Biol.* **20**, 126–136 (2008).
39. M. J. Spellberg, M. T. M. Ii, FOXO regulates RNA interference in Drosophila and protects from RNA virus infection. *Proc. Natl. Acad. Sci. U.S.A.* **112**, 14587–14592 (2015).
40. R. Yamamoto, M. Tatar, Insulin receptor substrate chico acts with the transcription factor FOXO to extend Drosophila lifespan. *Aging Cell* **10**, 729–732 (2011).
41. F. Demontis, N. Perrimon, Integration of Insulin receptor/Foxo signaling and dMyc activity during muscle growth regulates body size in Drosophila. *Development* **136**, 983–993 (2009).
42. F. C. G. Reis *et al.*, Fat-specific Dicer deficiency accelerates aging and mitigates several effects of dietary restriction in mice. *Aging (Albany. NY)* **8**, 1201–1222 (2016).
43. H. Herranz *et al.*, The miRNA machinery targets Mei-P26 and regulates Myc protein levels in the Drosophila wing. *EMBO J.* **29**, 1688–1698 (2010).
44. J. K. Park, X. Liu, T. J. Strauss, D. M. McKearin, Q. Liu, The miRNA pathway intrinsically controls self-renewal of Drosophila germline stem cells. *Curr. Biol.* **17**, 533–538 (2007).
45. S. Pinto *et al.*, Enoxacin extends lifespan of C. elegans by inhibiting miR-34-5p and promoting mitohormesis. *Redox Biol.* **18**, 84–92 (2018).
46. J. J. Forman, A. Legesse-Miller, H. A. Coller, A search for conserved sequences in coding regions reveals that the let-7 microRNA targets Dicer within its coding sequence. *Proc. Natl. Acad. Sci. U. S. A.* **105**, 14879–14884 (2008).
47. S. Tokumaru, M. Suzuki, H. Yamada, M. Nagino, T. Takahashi, let-7 regulates Dicer expression and constitutes a negative feedback loop. *Carcinogenesis* **29**, 2073–2077 (2008).
48. Y. S. Lee *et al.*, Distinct roles for Drosophila Dicer-1 and Dicer-2 in the siRNA/miRNA silencing pathways. *Cell* **117**, 69–81 (2004).
49. C. Slack, M. E. Giannakou, A. Foley, M. Goss, L. Partridge, dFOXO-independent effects of reduced insulin-like signaling in Drosophila. *Aging Cell* **10**, 735–748 (2011).
50. A. H. Brand, N. Perrimon, Targeted gene expression as a means of altering cell fates and generating dominant phenotypes. *Development* **118**, 401–15 (1993).
51. S. B. Pierce *et al.*, dMyc is required for larval growth and endoreplication in Drosophila. *Development* **131**, 2317–27 (2004).
52. J. Schindelin *et al.*, Fiji: an open-source platform for biological-image analysis. *Nat. Methods* **9**, 676–682 (2012).
53. T. D. Schmittgen *et al.*, Real-time PCR quantification of precursor and mature microRNA. *Methods* **44**, 31–38 (2008).
54. S. G. Landt *et al.*, ChIP-seq guidelines and practices of the ENCODE and modENCODE consortia. *Genome Res.* **22**, 1813–31 (2012).